SCIENTIFIC REPORTS

OPEN

Dark trions and biexcitons in WS_2 and WSe_2 made bright by e-e scattering

Received: 10 January 2017
Accepted: 07 March 2017
Published: 06 April 2017

Mark Danovich, Viktor Zólyomi & Vladimir I. Fal'ko

The direct band gap character and large spin-orbit splitting of the valence band edges (at the K and K′ valleys) in monolayer transition metal dichalcogenides have put these two-dimensional materials under the spot-light of intense experimental and theoretical studies. In particular, for Tungsten dichalcogenides it has been found that the sign of spin splitting of conduction band edges makes ground state excitons radiatively inactive (dark) due to spin and momentum mismatch between the constituent electron and hole. One might similarly assume that the ground states of charged excitons and biexcitons in these monolayers are also dark. Here, we show that the intervalley ($K \leftrightarrows K'$) electron-electron scattering mixes bright and dark states of these complexes, and estimate the radiative lifetimes in the ground states of these "semi-dark" trions and biexcitons to be ~10 ps, and analyse how these complexes appear in the temperature-dependent photoluminescence spectra of WS_2 and WSe_2 monolayers.

The truly 2D nature of TMDCs[1–7] enhances the effects of Coulomb interaction[8,9], resulting in charge complexes such as excitons[10–13], trions[13] and biexcitons[14] with binding energies that are orders of magnitude larger compared to conventional semiconductors such as GaAs. These complexes, which dominate the optical response of these materials, are comprised of spin/valley polarised electrons and holes residing at the corners K and K′ of the hexagonal Brillouin zone (BZ), where the selection rules of optical transitions require the same spin and valley states of the involved electrons at the conduction and valence band edges. As a result, the opposite spin projections of the conduction (c) and valence (v) band edges, found in monolayers of WS_2 and WSe_2, makes ground state excitons in these 2D crystals dark[15,16], so that their radiative transition would require help from defects, phonons[17] or magnetic field[18,19].

Applying the spin and valley selection rules to ground state trions and biexcitons might imply that these charge complexes are dark, too. In the 'dark' (d) state both electrons are in the bottom spin-orbit split states of c-band, whereas in the state to be 'bright' (b), one of the electrons has to be in the excited spin-split state. Here, we show that an intervalley scattering[20,21] of the c-band electrons mixes dark and bright states of complexes (Fig. 1), hence transferring some optical strength from b- to d-states and making dark state 'semi-dark'. For the resulting recombination line of such semi-dark complexes, we find that it is shifted downwards in energy (relative to the bright trion line) by $2\Delta_{SO}$, twice the c-band spin-orbit splitting.

With the reference to Fig. 1, the basis of trion, T (biexciton, B) states, $T^{\sigma_v\tau_v}_{\sigma_c\tau_c\sigma_{c'}\tau_{c'}}\left(B^{\sigma_v\tau_v\sigma_{v'}\tau_{v'}}_{\sigma_c\tau_c\sigma_{c'}\tau_{c'}}\right)$, can be described by spin, $\sigma = \uparrow, \downarrow$ and valley, $\tau = K, K'$ quantum numbers of their constituent c- and v-band states. In these notations, dark ground state exciton complexes T_d (B_d) are $T^{\uparrow K}_{\downarrow K,\uparrow K'}$ and $T^{\downarrow K'}_{\downarrow K,\uparrow K'}$ ($B^{\uparrow K,\downarrow K'}_{\downarrow K,\uparrow K'}$), and the excited states $T^{\uparrow K}_{\uparrow K,\downarrow K'}$ and $T^{\downarrow K'}_{\uparrow K,\downarrow K'}$ ($B^{\uparrow K,\downarrow K'}_{\uparrow K,\downarrow K'}$) are bright, T_b (B_b) (Supplementary material S1). These states are mixed by the intervalley interaction illustrated by a sketch in Fig. 1

$$H_{iv} = \frac{\hbar^2\chi}{2m_c}\sum_{\sigma,\tau}\int d^2\vec{r}\,\Psi^{\dagger}_{c,\sigma,-\tau}(\vec{r})\Psi^{\dagger}_{c,-\sigma,\tau}(\vec{r})\Psi_{c,-\sigma,-\tau}(r)\Psi_{c,\sigma,\tau}(\vec{r}). \quad (1)$$

Here, $\Psi_{c,\sigma,\tau}(\vec{r})$ are the conduction band electron field operators. The large momentum transfer between two electrons changing their valley states is determined by their Coulomb interaction at the unit cell scale, parametrised by a dimensionless factor χ. We estimate the size of this factor using both a tight-binding model and density functional theory (DFT). For the tight-binding model, we use the DFT calculated orbital decomposition

National Graphene Institute, University of Manchester, Booth St E, Manchester M13 9PL, UK. Correspondence and requests for materials should be addressed to M.D. (email: mark.danovich@postgrad.manchester.ac.uk)

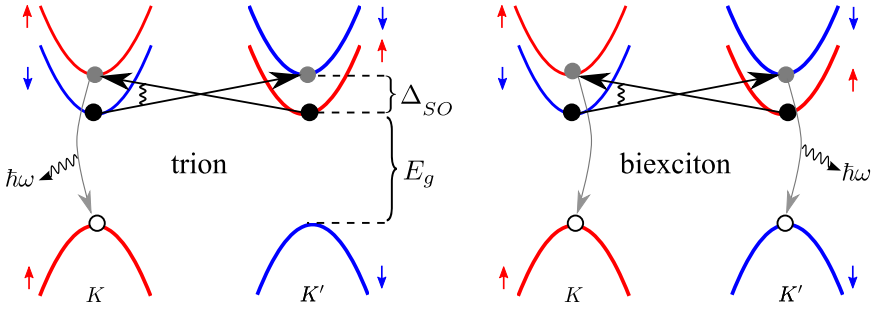

Figure 1. Intervalley electron-electron scattering process. Schematics of the band structures of WX_2 near the K, K' points of the BZ, and the intervalley scattering process that mixes dark and bright states of trions (T) and biexcitons (B). E_g is the band gap and Δ_{SO} stands for the conduction band spin splitting. Due to the large spin-orbit splitting in the valence band, the valence band is shown only for the higher-energy spin-polarised states.

	χ_{DFT}	χ_{TB}	μ_T [meV]	μ_B [meV]	τ_X [ps]	$\tau_{sd}(T)$ [ps]	$\tau_{sd}(B)$ [ps]
WS_2	1.0	1.6	18[29]	8.6[13]	0.25	7.8[3.9]	15[7.0]
WSe_2	1.3	2.0	19[30]	9.2[14]	0.26	9.4[4.7]	18[8.0]

Table 1. Scattering matrix elements and radiative lifetimes. Listed are the Intervalley scattering parameter χ calculated using DFT and tight binding (TB) model and the corresponding trion and biexciton mixing parameters $\mu T/B$ obtained using the electron-electron contact pair densities calculated in ref. 24 using diffusion quantum Monte Carlo, shown as DFT [TB], and the radiative lifetimes of the bright exciton, semi-dark trion and biexciton.

to construct the Bloch states at the Brillouin zone corners, and we use a 3D Coulomb potential for the interaction between electrons. As the c-band states at the K/K' points are primarily composed[6,7] of the metal $5d_{z^2}$ orbitals centred at the lattice sites $\vec{R}$ of metallic atoms in TMDC lattice, $\phi(\vec{r}-\vec{R})$, which we use to construct the tight-binding model Bloch states, to find

$$\chi = \frac{m_c}{m}\frac{A}{a_B}|C|^4\sum_{\vec{R}} e^{i\vec{K}\cdot\vec{R}}\int d^3\vec{r}_1 d^3\vec{r}_2 \frac{|\phi(\vec{r}_1)|^2|\phi(\vec{r}_2)|^2}{|\vec{r}_2-\vec{r}_1+\vec{R}|}. \tag{2}$$

Here, $\vec{K}=\left(\frac{4\pi}{3a_0},\ 0\right)$ with a_0 the lattice constant of WX_2, $A=\frac{\sqrt{3}}{2}a_0^2$ is the unit cell area, m_c is the c-band electron effective mass, m is the free electron mass, a_B is the Bohr radius, and C is the transition metal $5d_{z^2}$ orbital amplitude in the c-band edge at the K point (supplementary material S2.2). Similarly, we evalutaed χ from wave functions obtained using DFT implemented in the local density approximation and VASP[22] code (neglecting spin-orbit coupling). We used a plane-wave basis corresponding to 600 eV cutoff energy and a 12×12 grid of k-points in the 2D Brillouin zone. We also had to employ periodic boundary conditions in the z-direction; for this reason we used a large inter-layer distance of 20 Å to mimic the limit of an isolated monolayer. The form factor was calculated by post-processing the DFT wave functions, by taking the matrix element of the bare Coulomb interaction between the initial and final states of the scattering process (see supplementary material S2.1). These two calculations have returned values of the intervalley scattering factor χ, as listed in Table 1. In the basis of $[|d\rangle;\ |b\rangle]$ of dark and bright states of trions, $[T^{\uparrow K}_{\downarrow K,\uparrow K'};\ T^{\uparrow K}_{\uparrow K,\downarrow K'}]$ and $[T^{\downarrow K'}_{\downarrow K,\uparrow K'};\ T^{\downarrow K'}_{\uparrow K,\downarrow K'}]$, or biexcitons $[B^{\uparrow K,\downarrow K'}_{\downarrow K,\uparrow K'};\ B^{\uparrow K,\downarrow K'}_{\uparrow K,\downarrow K'}]$, the coupling in equation (1) leads to the mixing described by a 2×2 matrix

$$\begin{aligned}
H &= \begin{pmatrix} E_b^{T/B} & \mu_{T/B} \\ \mu^*_{T/B} & E_d^{T/B}\end{pmatrix},\quad \mu_T=\frac{\hbar^2\chi}{m_c}g_T,\quad \mu_B=\frac{\hbar^2\chi}{m_c}g_B,\\
E_b^T &= 2E_g+2\Delta_{SO}-\varepsilon_X-\varepsilon_T+\delta',\\
E_d^T &= 2E_g-\varepsilon_X-\varepsilon_T+\delta,\\
E_b^B &= 2E_g+2\Delta_{SO}-\varepsilon_X-\varepsilon_B+2\delta',\\
E_d^B &= 2E_g-\varepsilon_X-\varepsilon_B+2\delta.
\end{aligned} \tag{3}$$

Where E_g is the band gap, ε_X, ε_T, and ε_B are the exciton, trion, and biexciton binding energies, respectively, and δ, δ' stand for the intravalley and intervalley electron-hole exchange[23], $\delta\approx6$ meV, which we will neglect in the following calculations. Note that the effective masses of the c-band spin split bands differ by[7] ~30–40% with the lower bands having the higher effective electron mass. This results in slightly higher binding energies for the dark

	$\frac{m_c}{m}$ [7]	$\frac{m_v}{m}$ [7]	Δ_{SO} [7] [meV]	A [7] [Å^2]	r_* [15] [nm]	E_{X_b} [28] [eV]	ε_T [29] [meV]	ε_B [29] [meV]	$\frac{v}{c}$ [7]
WS_2	0.26	−0.35	32	8.65	3.8	2	34	24	1.7×10^{-3}
WSe_2	0.28	−0.36	37	9.38	4.5	1.7	31	20	1.6×10^{-3}

Table 2. Material parameters. Listed are the effective c- and v-band electron masses m_c and m_v, c-band spin-orbit splitting Δ_{SO}, unit cell area A, 2D screening length r_*, bright exciton energy E_{X_b}, trion binding energy ε_T, biexciton binding energy ε_B, and the velocity related to the off diagonal momentum matrix element relative to the speed of light v/c.

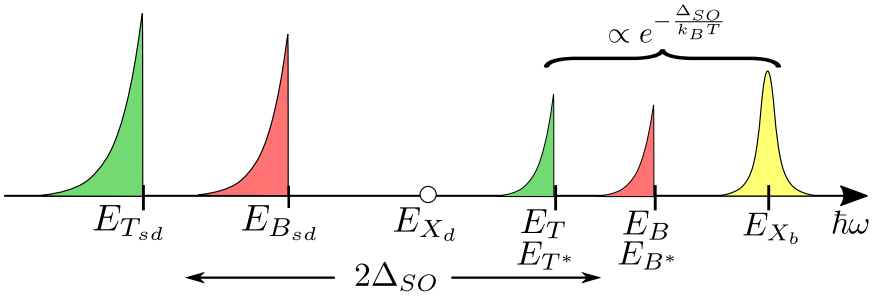

Figure 2. Low temperature photoluminescence spectrum of WX_2. Sketch of the low temperature ($k_BT < \Delta_{SO}$) photoluminescence spectrum of WX_2 including the bright exciton, dark and bright trions (green) and dark and bright biexcitons (red). The excited bright trions and excitons are denoted by T^* and B^*. The dark exciton (X_d) energy is marked as a reference point $E_{X_d} = E_{X_b} - \Delta_{SO}$.

ground state charge complexes compared to the excited states, resulting in a larger value for their energy difference $E_b - E_d$. The mixing parameter $\mu \equiv \langle b|H_{iv}|d\rangle = \frac{\hbar^2\chi}{m_c}\int\prod_i d^2\vec{r}_i\,|\Phi_{T/B}|^2\,\delta\left(\vec{r}_e - \vec{r}_{e'}\right)$, (where $\Phi_{T/B}$ stands for the wave function of the trion or biexciton and $i = e, e', h, (h')$, is determined by the electron-electron contact pair densities[24] in the trion, g_T and biexciton, g_B. The mixing of the dark and bright states results in a slight shift of their energies and, most importantly, in a finite radiative decay rate, τ_{sd}^{-1} of the semi-dark (sd) trions (T) and biexcitons (B),

$$\begin{aligned}\frac{1}{\tau_{sd}} &\approx \left(1 - \frac{1}{\sqrt{1+\left(\frac{\mu_{T/B}}{\Delta_{SO}}\right)^2}}\right)\frac{\alpha_{T/B}}{2}\tau_X^{-1},\\ \frac{1}{\tau_X} &= \frac{8\pi}{\hbar}\frac{e^2}{\hbar c}\frac{\hbar^2v^2}{E_{X_b}}\,|\Phi_X(0)|^2,\end{aligned} \tag{4}$$

where τ_X^{-1} is the radiative decay rate of the bright exciton[25–27], determined by the electron-hole overlap factor $|\Phi_X(0)|^2$ ($\Phi_X(r_{eh})$ is the envelope wave function describing relative motion of the electron and hole in the exciton), v is the velocity related to the off diagonal momentum matrix element. The values of the factors $\alpha_T = \frac{1}{2}$ and $\alpha_B = 1$ have been estimated based on the following consideration (see supplementary material S3). As the exciton's binding energy is significantly larger than that of the trion or biexciton, these bound complexes can be viewed as strongly-bound, with an additional weakly bound electron in the case of a trion, or an exciton in the case of a biexciton. For a trion, this results in a reduction of the recombining electron-hole contact pair density by a factor of two as compared to the exciton, as the hole is shared between the two electrons such that the recombining electron (which has the right spin projection), will be near it only half of the time. In the case of the biexciton, each electron spends half of the time near its hole with which it can recombine, and half of the time near the other hole. As there are two excitons able to recombine we get $\alpha_B = 1$. The resulting values for the lifetimes (using the material parameters in Table 2) are summarized in Table 1.

The mixing of the dark and bright states produces photoluminescence lines shown schematically in Fig. 2. The emitted photon energies of these lines are determined by both the binding energies and the shake-up into the higher-energy spin-split c-band in the final state,

$$\begin{aligned} E_{X_b} &= E_g + \Delta_{SO} - \varepsilon_X, \\ E_{T_{sd}/B_{sd}} &\approx E_{X_b} - \varepsilon_{T/B} - 2\Delta_{SO}, \\ E_{T/B} &\approx E_{X_b} - \varepsilon_{T/B}, \end{aligned} \tag{5}$$

Being the ground states, the semi-dark trion and biexcitons (T_{sd}, B_{sd}) do not require an activation and therefore should appear in the spectrum even at low temperatures. In contrast, the bright states do require thermal activation, resulting in a $e^{-\Delta E/k_B T}$ temperature dependence of their lines intensities. For the bright exciton, trion $[T^{\uparrow K}_{\uparrow K,\uparrow K'};\ T^{\downarrow K'}_{\downarrow K,\downarrow K'}]$ and biexciton $[B^{\uparrow K,\downarrow K'}_{\uparrow K,\uparrow K'};\ B^{\uparrow K,\downarrow K'}_{\downarrow K,\downarrow K'}]$ we have $\Delta E \approx \Delta_{SO}$, while for the excited mixed dark and bright trion (T^*) $[T^{\uparrow K}_{\uparrow K,\downarrow K'};\ T^{\downarrow K'}_{\uparrow K,\downarrow K'}]$ and biexciton (B^*) $B^{\uparrow K,\downarrow K'}_{\uparrow K,\downarrow K'}$, $\Delta E \approx 2\Delta_{SO}$. Also, the presence of a final state electron or exciton results in an antisymmetric line shape with a cutoff due to the recoil kinetic energy of the remaining electron or exciton that shifts the emission line to a lower energy. A typical recoil kinetic energy is $\frac{m_X}{m_c} k_B T$ for the trions and $k_B T$ for biexcitons, with k_B the Boltzmann constant, m_X the exciton mass, and m_c the c-band electron effective mass.

In conclusion, we have shown that intervalley electron-electron scattering makes "dark" ground state trions and biexcitons in Tungsten dichalcogenides WS_2 and WSe_2 optically active, with a lifetime $\tau_{T/B} \sim 10$ ps, to compare with a sub-ps lifetime of bright excitons in 2D TMDCs.

References

1. Wang, H. Q., Kalantar-Zadeh, K., Kis, A., Coleman, J. N. & Strano, M. S. Electronics and optoelectronics of two-dimensional transition metal dichalcogenides. *Nat. Nanotechnol.* **7(11),** 699–712 11 (2012).
2. Cao, T. *et al.* Valley-selective circular dichroism of monolayer molybdenum disulphide. *Nat. Commun.* **3,** 887 06 (2012).
3. Xiao, D., Liu, G. B., Feng, W., Xu, X. & Yao, W. Coupled spin and valley physics in monolayers of MoS_2 and other group-vi dichalcogenides. *Phys. Rev. Lett.* **108,** 196802 (May 2012).
4. Jones, A. M. *et al.* Optical generation of excitonic valley coherence in monolayer wse_2. *Nat Nano* **8(9),** 634–638 09 (2013).
5. Zeng, H., Dai, J., Yao, W., Xiao, D. & Cui, X. Valley polarization in MoS_2 monolayers by optical pumping. *Nat Nano* **7(8),** 490–493 08 (2012).
6. Liu, G. B., Xiao, D., Yao, Y., Xu, X. & Yao, W. Electronic structures and theoretical modelling of two-dimensional group-vib transition metal dichalcogenides. *Chem. Soc. Rev.* **44,** 2643–2663 (2015).
7. Kormanyos, A. *et al.* k. p theory for two-dimensional transition metal dichalcogenide semiconductors. *2D Materials* **2(2),** 022001 (2015).
8. Chernikov, A. *et al.* Exciton binding energy and nonhydrogenic rydberg series in monolayer WS_2. *Phys. Rev. Lett.* **113,** 076802 (Aug 2014).
9. Cudazzo, P., Tokatly, I. V. & Rubio, A. Dielectric screening in two-dimensional insulators: Implications for excitonic and impurity states in graphane. *Phys. Rev. B.* **84,** 085406 (Aug 2011).
10. Mak, K. F. *et al.* Tightly bound trions in monolayer MoS_2. *Nat Mater* **12(3),** 207–211 03 (2013).
11. Qiu, D. Y., da Jornada, F. H. & Louie, S. G. Optical spectrum of MoS_2: Many-body effects and diversity of exciton states. *Phys. Rev. Lett.* **111,** 216805 (Nov 2013).
12. Ramasubramaniam, A. Large excitonic effects in monolayers of molybdenum and tungsten dichalcogenides. *Phys. Rev. B.* **86,** 115409 (Sep 2012).
13. Berkelbach, T. C., Hybertsen, M. S. & Reichman, D. R. Theory of neutral and charged excitons in monolayer transition metal dichalcogenides. *Phys. Rev. B.* **88,** 045318 (Jul 2013).
14. You, Y. *et al.* Observation of biexcitons in monolayer WSe_2. *Nat Phys* **11(6),** 477–481 06 (2015).
15. Echeverry, J. P., Urbaszek, B., Amand, T., Marie, X. & Gerber, I. C. Splitting between bright and dark excitons in transition metal dichalcogenide monolayers. *Phys. Rev. B.* **93,** 121107 (Mar 2016).
16. Zhang, X. X., You, Y., Yang, S., Zhao, F. & Heinz, T. F. Experimental evidence for dark excitons in monolayer WSe_2. *Phys. Rev. Lett.* **115,** 257403 (Dec 2015).
17. Danovich, M., Zólyomi, V., Fal'ko, V. I. & Aleiner, I. L. Auger recombination of dark excitons in ws_2 and wse_2 monolayers. *2D Materials* **3(3),** 035011 (2016).
18. Zhang, X. X. *et al.* Magnetic brightening and control of dark excitons in monolayer WSe_2. cond-mat/1612.03558v1 (2016).
19. Molas, M. R. *et al*. Brightening of dark excitons in monolayers of semiconducting transition metal dichalcogenides. cond-mat/1612.02867v1 *2D materials*, **4(2)**, 021003 (2017).
20. Yu, H., Cui, X., Xu, X. & Yao, W. Valley excitons in two-dimensional semiconductors. *National Science Review* **2(1),** 57–70 (2015).
21. Dery, H. Theory of intervalley coulomb interactions in monolayer transition-metal dichalcogenides. *Phys. Rev. B.* **94,** 075421 (Aug 2016).
22. Kresse, G. & Furthmüller, J. Efficient iterative schemes for *ab initio* total-energy calculations using a plane-wave basis set. *Phys. Rev. B.* **54,** 11169–11186 (Oct 1996).
23. Plechinger, G. *et al.* Trion fine structure and coupled spin-valley dynamics in monolayer tungsten disulfide. *Nat Commun* **7,** 09 (2016).
24. Syniszewski, M., Mostaani, E., Drummond, N. D., Aleiner, I. & Fal'ko, V. I. Binding energies of trions and biexcitons in two-dimensional semiconductors from diffusion quantum Monte Carlo calculations. *Phys. Rev. B.* **95,** 081301 (Feb 2017).
25. Palummo, M., Bernardi, M. & Grossman, J. C. Exciton radiative lifetimes in two-dimensional transition metal dichalcogenides. *Nano Letters* **15(5),** 2794–2800 (2015).
26. Slobodeniuk, A. O. & Basko, D. M. Spin-flip processes and radiative decay of dark intravalley excitons in transition metal dichalcogenide monolayers. *2D Materials* **3(3),** 035009 (2016).
27. Wang, H. *et al.* Radiative lifetimes of excitons and trions in monolayers of the metal dichalcogenide mos_2. *Phys. Rev. B.* **93,** 045407 (Jan 2016).
28. Hanbicki, A. T., Currie, M., Kioseoglou, G., Friedman, A. L. & Jonker, B. T. Measurement of high exciton binding energy in the monolayer transition-metal dichalcogenides ws_2 and wse_2. *Solid State Communications* **203,** 16–20 2 (2015).
29. Kylänpää, I. & Komsa, H. P. Binding energies of exciton complexes in transition metal dichalcogenide monolayers and effect of dielectric environment. *Phys. Rev. B.* **92,** 205418 (Nov 2015).

Acknowledgements

This work was supported by the EU Graphene Flagship Project, the Engineering and Physical Sciences Research Council (EPSRC, EP/N010345/1), and the European Research Council (ERC Synergy Grant Hetero2D). The authors would like to thank I. Aleiner, T. Heinz, M. Potemski, M. Syniszewski, A. Tartakovski and X. Xu for useful discussions.

Author Contributions

M.D. and V.F. wrote the main manuscript text. V.Z. performed the density functional calculations and wrote section S2.1 in the supplementary material. M.D. produced Figs 1, 2 and S2 in the supplementary material. All authors reviewed and improved the manuscript.

Additional Information

Supplementary information accompanies this paper at http://www.nature.com/srep

Competing Interests: The authors declare no competing financial interests.

How to cite this article: Danovich, M. *et al.* Dark trions and biexcitons in WS_2 and WSe_2 made bright by e-e scattering. *Sci. Rep.* **7**, 45998; doi: 10.1038/srep45998 (2017).

Publisher's note: Springer Nature remains neutral with regard to jurisdictional claims in published maps and institutional affiliations.